Full Paper

# In Situ Fabrication of Single Poly(methyl pyrrole) Nanowire

*Kumaran Ramanathan*,[a] *Mangesh A. Bangar*,[a] *Minhee Yun*,[b] *Wilfred Chen*,[a] *Ashok Mulchandani*,[a]* *Nosang V. Myung*[a]*

[a] Department of Chemical and Environmental Engineering, and Center for Nanoscale Science and Engineering, University of California, Riverside, CA 92521, USA
*e-mail: myung@engr.ucr.edu; adani@engr.ucr.edu
[b] Department of Electrical and Computer Engineering, University of Pittsburgh, Pittsburgh, PA 15261, USA

Received: October 13, 2006
Accepted: November 9, 2006

**Abstract**
One hundred nm wide by four μm long poly(methyl pyrrole) (PMPy) nanowires without and with biomolecule, biotin-quantum dot, were synthesized by electrochemical polymerization of 1-methyl pyrrole with chloride and *p*-toluene sulfonate dopants in nanochannels between microfabricated gold electrodes. Scanning electron microscopy examination revealed well-confined dendrite free chloride-doped PMPy nanowires with embedded biotin-quantum dot. Current vs. voltage investigation demonstrated ohmic nature of contact for all nanowires. Chloride-doped PMPy nanowires were more conductive than with *p*-toluene sulfonate doped PMPy nanowires whereas entrapment of biotin-quantum dot increased the conductivity.

**Keywords:** Poly(methyl pyrrole), Nanowire, Conducting polymer, Dopant, Biosensor

DOI: 10.1002/elan.200603773

## 1. Introduction

One-dimensional (1-D) nanostructures [1], such as nanowires [2–5], nanobelts, nanospring, nanotubes [6, 7], and metallic nanowires [8], are extremely attractive for (bio)-electronic detection because of a number of reasons. First, their high surface-to-volume ratio, together with novel electron transport properties of the 1-D nanostructures, give rise to large resistance/conductance changes in the nanostructures associated with the binding of molecules onto the surface of the nanostructures to potentially single-molecule detection [2]. Second, the direct conversion of chemical information into an electronic signal can take advantage of the existing low power microelectronic technology [9, 10] and lead to miniaturized sensor devices [11, 12]. Finally, the small size of the nanostructures makes it possible to develop high density arrays of individually addressable nanostructures for simultaneous analysis of a range of different species and massive redundancy to reduce false positive/negative.

Several groups have demonstrated that the conductance of nanotubes and nanowires are sensitive to the adsorption of different molecules. When functionalized with bioreceptors, label-free bioaffinity sensing can be achieved rapidly with extremely high sensitivity [2, 13]. However, finding a quick and reliable method to assemble a single, let alone many for high density arrays, nanowire and nanotube into a device and to connect them for electrical measurements has been a challenge. Additionally, because of harsh conditions used for synthesis of nanowires and nanotubes [14, 18], the modification with biomolecules can only be performed postsynthesis and positioning which also involves complex chemistries and harsh chemicals.

Conducting polymers [19–21] nanowires [22–25] such as polypyrrole (PPy), poly(methyl pyrrole) (PMPy), polyaniline (PANI) and polythiophene (PT) have many advantages compared to CNT and silicon nanowires. First, they exhibit electrical, magnetic, optical properties of metals or semiconductors while retaining the attractive mechanical properties and processing advantages of polymers. Their conductivity can be controllably varied from the insulating through the semiconducting to metallic regime by oxidizing (p-type doping) or reducing (n-type doping). Second, they are inexpensive, flexible, and air-stable. Third, they can be synthesized electrochemically, allowing an easy control of the initiation and termination of polymerization by simply switching the current on and off, respectively. Fourth, polymerization can be performed from benign aqueous environment in ambient conditions, making one-step synthesis of biologically-functionalized nanowires possible by the incorporation of biological molecules during the electrochemical polymerization. Fifth, a diversity of monomers, dopants and electropolymerization conditions can be used for designing nanowires of tailor-made properties such as conductivity, selectivity, porosity, etc. Finally, the electrodes used for electropolymerization are the built-in contacts for the subsequent biosensor measurements.

We recently reported a single step technique for the growth and entrapment of biomolecules (avidin-quantum dot conjugate or avidin) into conducting polypyrrole nanowire grown within 100 nm wide and 3 μm long channels between gold electrodes [26]. In the present article, we extended our effort to demonstrate the versatility of our fabrication method by electropolymerizing poly(methyl pyrrole) (PMPy) nanowires with an entrapped biomolecule

 

(i.e., Biotin conjugated quantum dot (Bqd)). PMPy was selected because it posses better electrochemical stability in oxidized states, greater mechanical strength, high anode activity and relatively low production cost compared to polypyrrole [27, 28].

The dopant anions (counter anions) in conducting polymer strongly influence physical properties including morphology, conductivity, dielectric constant, color, adhesion, and mechanical strength. A variety of anions ranging from inorganic such as chloride, perchlorate, and hydrogen sulfate, to organic such as *p*-toluene sulfonate, *p*-bromobenzene sulfonate, enzyme, anitobody and DNA have been utilized as dopants for conducting polymer electrosynthesis [29, 30]. In order to examine the effect of dopants, two different anions (i.e., chloride and *p*-toluene sulfonate (PTS)) were selected to investigate their effects on the conductivity and morphology of PMPy nanowires.

## 2. Experimental

The deposition and growth of the conducting polymer nanowire are based on well-known electrooxidative polymerization processes, wherein maintaining an optimal current flow between the anode and cathode, results in the initiation and growth of the conducting polymer from the anode, filling the gap between the two electrodes and establishing contact with the cathode. The procedure for growth of the PMPy nanowire or biomolecule entrapped PMPy nanowire is performed in a single step. The ability to grow arrays of similar conducting polymer nanowires was recently demonstrated [26, 31].

The platform for the growth of the conducting polymer nanowire is described elsewhere [4]. In a typical experiment, the silicon substrate with the e-beam patterned nanochannel on electrodes were mounted on a probe station and connected using contact pins to the contact pads of electrodes for the anode and cathode. A quasi Ag reference electrode was placed at an optimal distance between the electrodes and close to the channel. A 2 μL deaerated monomer solution (0.3 M 1-methyl pyrrole in 0.01 M KCl or 0.01 M PTS) was placed on the surface of the channel and its contact with the reference electrode was ascertained. A 0.2 μM solution of Bqd in 100 μL of methyl pyrrole electrolyte solution was used as the electrolyte solution to obtain biomolecule entrapped PMPy nanowire. The electropolymerization was initiated by applying a 100 nA current on the stationary drop of the monomer solution and the change in potential of the anode was monitored. In general the potential value rises to about 2.3 to 2.8 V vs. reference electrode from the open circuit potential, within 2 s after initiating the electropolymerization. Thereafter the potential remains constant or shows a gradual decrease until the nanowire contacts with the cathode. At the point of contact with the cathode the potential drops to approximately 0.0 V and the electropolymerization is stopped within 25 s after the contact. In this period the potential changes at the anode depend on the various electrode processes on its surface.

## 3. Results and Discussion

Figure 1A shows a typical chronopotentiogram for the deposition of chloride-doped PMPy-Bqd nanowire in 0.01 M KCl. The change in the anode potential was monitored as a function of time. The initial potential of 2.8 V was acquired within 1sec followed by a decline to a constant value of 2.5 V for 8 sec prior to dipping to 0.2 V. Thereafter the potential gradually reached to 0.0 V upon further electropolymerization. The sharp dip around 8 s demonstrates the establishment of the contact of the PMPy-Bqd nanowire with the cathode. The potential changes were controlled by the electrode processes during PMPy nanowire formation. A similar profile was also obtained for PMPy nanowire without Bqd (Fig. 1B). A potential of 2.5 V was achieved following application of the 100 nA current. Thereafter, the potential stabilized around 2.2 V and remained constant for about 12 sec prior to dipping to 0.0 V. Further, the potential remained constant.

In order to further verify the integrity and stability of the chloride-doped PMPy nanowires, current voltage ($I-V$) characteristics were performed. As shown in Figure 2A, the $I-V$ characteristics for the wet chloride-doped PMPy nanowire containing the Bqd was much steeper, showing a higher conductance as compared to the chloride-doped PMPy nanowire without the entrapped Bqd (Fig. 2B). The higher conductance of the Bqd entrapped PMPy nanowire may perhaps be due to the participation of the semiconducting nanoparticles (Bqd) in the conductivity processes. In this instance the quantum dots (ZnS coated CdSe nanoparticles) were conjugated to the biotin molecule using a polymeric support layer.

The linear change in the current with potential shows the ohmic nature of the contact between the chloride-doped PMPy nanowire and the gold electrodes. This also demonstrates that the nanowire behaves like a typical metallic nanowire, and obeys ohms law, with negligible contact resistance between the PMPy nanowire and gold electrodes.

A similar investigation was performed with *p*-toluene sulfonate (PTS) doped PMPy to investigate the effect of sulfonate ion doping on nanowire morphology and conductivity. Figure 3A shows a typical chronopotentiogram for the deposition of PTS-doped PMPy-Bqd in 0.01 M PTS. The PTS-doped PMPy-Bqd was obtained within 46 s upon passage of current. Following the nanowire formation the potential was stable at 0.0 V for about 22 s before the deposition process was stopped. This demonstrates the integrity and stability of the Bqd embedded PMPy nanowire after formation. The profile for PTS-doped PMPy without Bqd (Fig. 3B) was similar. The nanowire was formed within 9 s and the potential remained around 0.0 V for more than 26 s, demonstrating the integrity and stability of PTS-doped PMPy nanowire.

Wet $I-V$ characterization of PTS-doped PMPy nanowires with entrapped Bqd showed a slightly higher conductance (Fig. 4A) when compared to without the entrapped Bqd (Fig. 4B). An earlier report [28] had examined the compatibility in size between of PTS and pyrrole leading to a

 

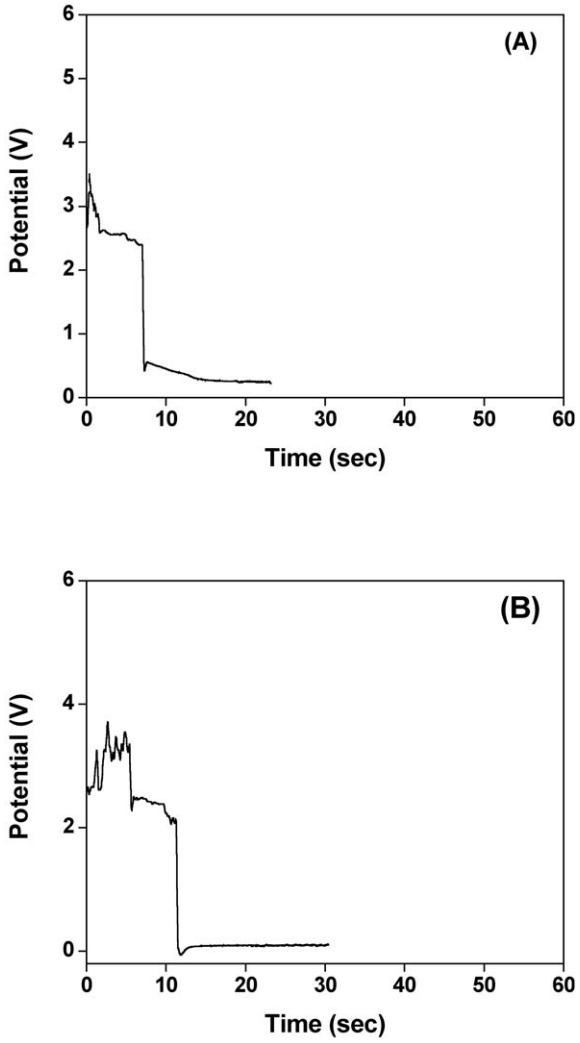


Fig. 1. The chronopotentiograms of chloride-doped PMPy nanowires with Bqd (A) and without Bqd (B). The electropolymerization solutions contain 0.3 M MPy in 0.01 M KCl with 0.2 μM Bqd (A) and without Bqd (B). The applied current was 100 nA on a 2 μL drop placed on the channel.

closer interaction and hence serving as an "ordering" element for the polypyrrole chains, providing the flexible properties of the nanowire. The preferential incorporation of PTS probably leads to a lesser incorporation of Bqd, thereby resulting in a lower conductance value. The native PTS-doped PMPy nanowires had a lower conductance compared to the chloride-doped PMPy nanowires. Similar results have been reported in thin films where the conductivity and specific gravity decreased with increase in anion size [32]. In addition, the change in conductance in the presence of Bqd was higher in chloride-doped PMPy compared to PTS-doped PMPy, perhaps due to a higher Bqd incorporation.

The confinement and uniformity of the chloride-doped PMPy-Bqd nanowire was further confirmed by the SEM and high resolution optical image (Fig. 5A) [33]. The well

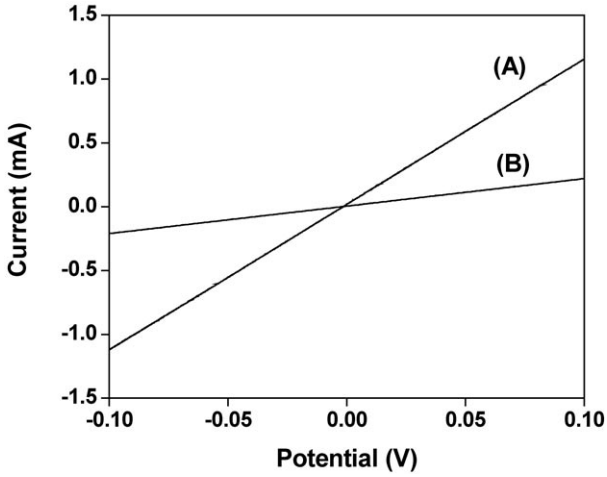


Fig. 2. The wet Current versus voltage ($I-V$) characteristics recorded on 100 nm PMPy nanowires with Bqd (A) and native PMPy (B) at a scan rate of 50 mV/s.

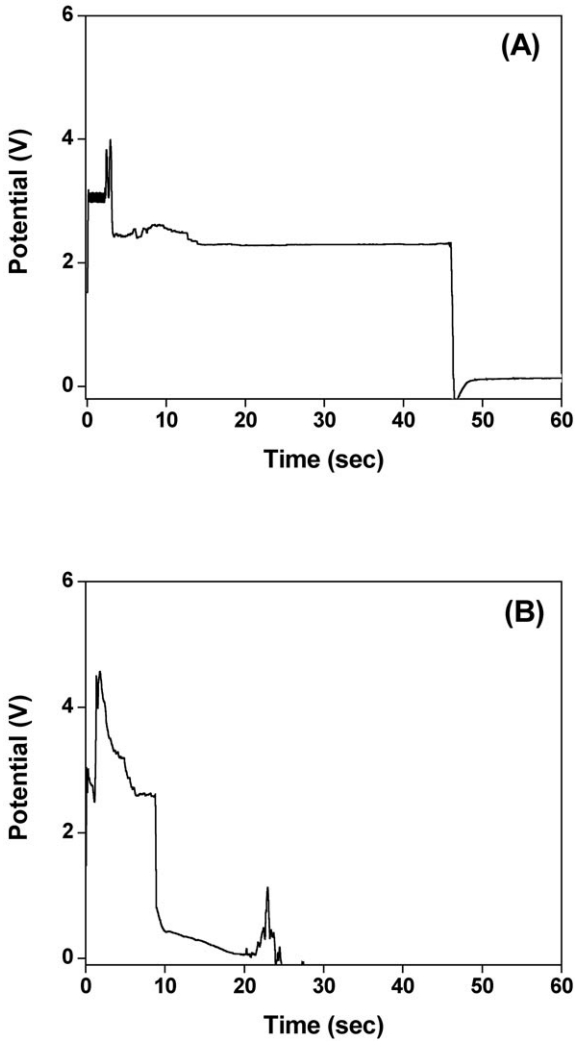


Fig. 3. The chronopotentiograms of PTS-doped PMPy nanowires with Bqd (A) and without Bqd (B). The electropolymerization solutions contain 0.3 M MPy in 0.01 M PTS with 0.2 μM Bqd (A) and without Bqd (B). The applied current was 100 nA on a 2 μL drop placed on the channel.

 

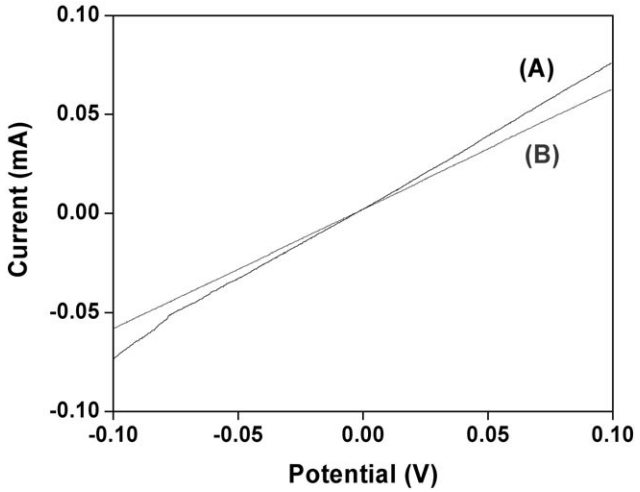


Fig. 4. The wet current versus voltage ($I-V$) characteristics recorded on 100 nm PTS-doped PMPy nanowires with Bqd (A) and without Bqd (B) at a scan rate of 50 mV/s.

confined nanowire within the 100 nm channel is clearly observed. However, PTS-doped PMPy-Bqd nanowire showed a poorly defined porous nanowire (Fig. 5B). The presence of the Bqd within the chloride-doped PMPy nanowire was verified by the presence of the Cd peak in the EDS analysis (Fig. 5C). In addition to the Cl peak from the dopant, the Si and Au peaks from the substrate are also observed.

## 4. Conclusions

We demonstrated electrochemically controlled single step growth and biomolecular functionalization of a 100 nm wide 4 micron long PMPy nanowire between microfabricated gold electrodes. Two different anions (i.e., inorganic chloride and organic *p*-toluene sulfonate (PTS)) were examined as dopants to investigate their effects on the conductivity and morphology of PMPy nanowires. The morphology and conductance of MPPy nanowires were strongly influenced by dopant types. Chloride-doped PMPy nanowires were well-confined within nanochannel and uniform with greater conductance than PTS-doped PMPy. In addition, the change in conductance in the presence of Bqd was greater in chloride-doped PMPy compared to PTS-doped PMPy, which might be due to a higher Bqd incorporation.

## 5. Acknowledgements

We acknowledge the support of this work by grants H94003-04-2-0404 from DOD/DARPA/DMEA, BES-0529330 from NSF and GR-83237501 from U.S. EPA. M. A. Bangar acknowledges the financial support from UC Graduate Researcher and Education in Adaptive Bio-Technology Training (GREAT) program.

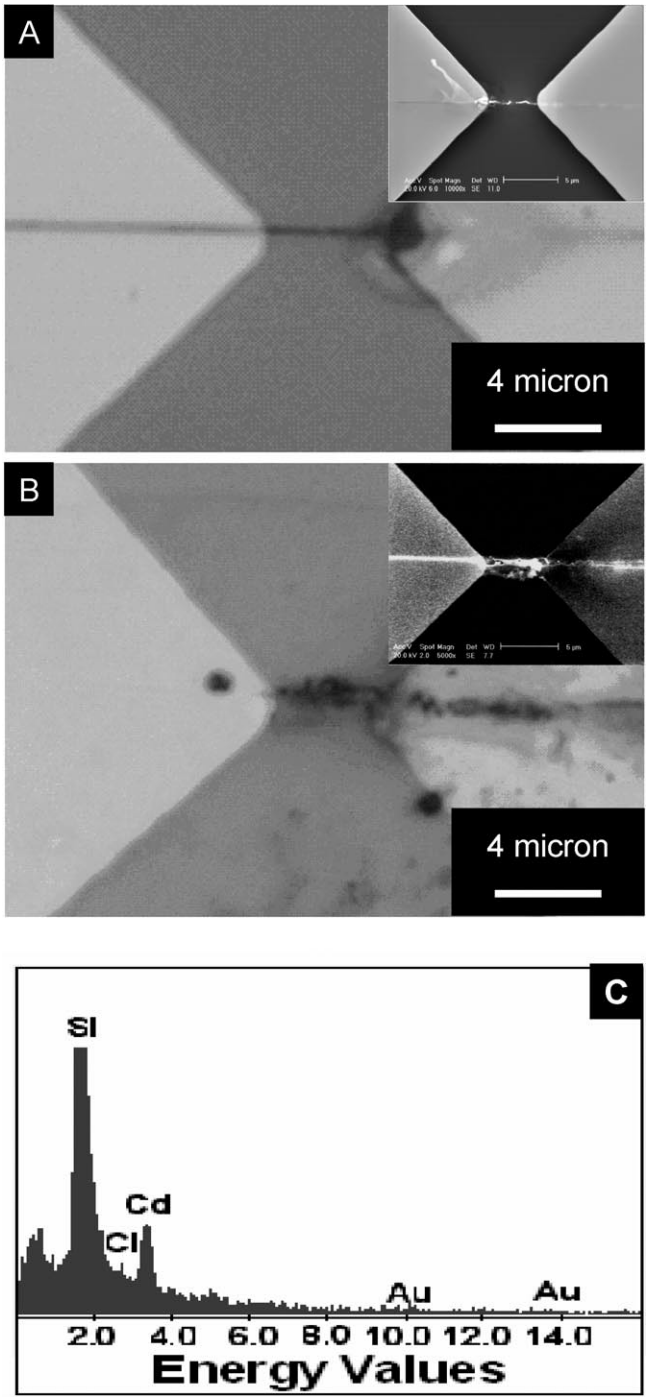


Fig. 5. A) The optical and SEM images of the chloride-doped PMPy-Bqd nanowire, B) the optical and SEM image of the PTS-doped PMPy-Bqd nanowire, and C) the EDS profile of a chloride-doped PMPy nanowire with embedded Bqd.

## 6. References

[1] A. F. Morales, C. M. Lieber, *Science* **1998**, *279*, 208.
[2] Y. Cui, Q. Wei, H. Park, C. M. Lieber, *Science* **2001**, *293*, 1289.
[3] Y. Huang, X. Duan, Q. Wei, C. M. Lieber, *Science* **2001**, *291*, 630.

 

[4] K. Yun, N. V. Myung, R. P. Vasquez, C. Lee, E. Menke, R. M. Penner, *Nano Lett.* **2004**, *4*, 419.
[5] R. J. Chen, S. Bangaruntip, K. A. Drouvalakis, N. W. S. Kam, M. Shim, L. Yiming, W. Kim, P. J. Utz, H. Dai, *PNAS* **2003**, *1000*, 4984.
[6] L. Roschier, J. Pentilla, M. Martin, P. Hakonen, M. Paalanen, U. Tapper, E. I. Kauppinen, C. Journet, P. Bernier, *Appl. Phys. Lett.* **1999**, *75*, 728.
[7] S. J. Tans, A. R. M. Verscheren, C. Dekker, *Nature* **1998**, *393*, 49.
[8] M. A. Bangar, K. Ramanathan, C. Hangarter, M. Yun, C. Lee, N. V. Myung, *Chem. Mater* **2004**, *16*, 4955.
[9] A. Bachtold, P. Hadley, T. Nakanishi, C. Dekker, *Science* **2001**, *294*, 1317.
[10] T. Rueckes, K. Kim, E. Joselevich, G. Y. Tseng, C. L. Cheung, C. M. Lieber, *Science* **2000**, *289*, 94.
[11] J. Kong, N. R. Franklin, C. W. Zhou, M. G. Chapline, S. Peng, K. J. Cho, H. J. Dai, *Science* **2000**, *287*, 622.
[12] S. Virji, J. X. Huang, R. B. Kaner, B. H. Weiller, *Nano Lett.* **2004**, *4*, 491.
[13] A. Star, J. C. P. Gabriel, K. Bradley, G. Gruner, *Nano Lett.* **2003**, *3*, 459.
[14] H. J. Dai, *Acc. Chem. Res.* **2002**, *35*, 1035.
[15] R. Andrews, D. Jacques, D. Qian, T. Rantell, *Acc. Chem. Res.* **2002**, *35*, 1008.
[16] J. T. Hu, T. W. Odom, C. M. Lieber, *Acc. Chem. Res.* **1999**, *32*, 435.
[17] L. C. Venema, J. W. G. Wildoer, H. L. J. T. Tuinstra, C. Dekker, A. G. Rinzler, R. E. Smalley, *Appl. Phys. Lett.* **1997**, *71*, 2629.
[18] A. Bezryadin, A. R. M. Verscheren, S. J. Tans, C. Dekker, *Phys. Rev. Lett.* **1998**, *80*, 4036.
[19] H. Shirakawa, *Angew. Chem., Int. Ed.* **2001**, *40*, 2575.
[20] A. J. Heeger, *Angew. Chem., Int. Ed.* **2001**, *40*, 2591.
[21] A. G. MacDiarmid, *Angew. Chem., Int. Ed.* **2001**, *40*, 2581.
[22] R. M. Hernandez, L. Richter, S. Semanick, S. Stranick, T. E. Mallouk, *Chem. Mater.* **2004**, *16*, 3431.
[23] J. Huang, S. Virji, B. H. Weiller, R. B. Kaner, *Chem. Eur. J.* **2004**, *10*, 1314.
[24] H. Q. Zhang, S. Boussaad, N. Ly, N. J. Tao, *Appl. Phys. Lett.* **2004**, *84*, 133.
[25] H. Q. Liu, J. Kameoka, D. A. Czaplewski, H. G. Craighead, *Nano Lett.* **2004**, *4*, 671.
[26] K. Ramanathan, M. A. Bangar, M. Yun, W. Chen, A. Mulchandani, N. V. Myung, *JACS* **2005**, *127*, 496.
[27] E. M. Genies, A. A. Syed, *Synth. Met.* **1984**, *10*, 21.
[28] K. Kaeriyama, M. Sato, K. Hamada, *Makromol. Chem., Rapid Commun.* **1989**, *10*, 171.
[29] J.-C. Vidal, E. Garcia-Ruiz, J.-R. Castillo, *Microchim. Acta.* **2003**, *143*, 93.
[30] A. K. Wanekya, W. Chen, N. V. Myung, A. Mulchandani, *Electroanalysis* **2006**, *18*, 533.
[31] K. Ramanathan, M. A. Bangar, M. Yun, W. Chen, A. Mulchandani, N. V. Myung, *Nano Lett.* **2004**, *4*, 1237.
[32] M. Yamaura, K. Sato, T. Hagiwara, Iwata., *Synth. Met.* **1992**, *48*, 337.
[33] Note: During the SEM imaging of the chloride-doped PMPy nanowire (Fig. 5A) a break in the nanowire occurred as observed almost at the center of the nanowire.

 